Cold-Field Switching in PVDF-TrFE Ferroelectric Polymer Nanomesas

Igor Stolichnov, Peter Maksymovych, Evgeny Mikheev, Sergei V. Kalinin, Alexander K. Tagantsev, and Nava Setter

Cold-field switching in PVDF-TrFE ferroelectric polymer nanomesas

Igor Stolichnov[1*], Peter Maksymovych[2], Evgeny Mikheev[1], Sergei V. Kalinin[2],

Alexander K. Tagantsev[1], Nava Setter[1]

* E-mail: igor.stolitchnov@epfl.ch

[1] Ceramics Laboratory, EPFL-Swiss Federal Institute of Technology,

Lausanne 1015, Switzerland

[2] Center for Nanophase Materials Science, Oak Ridge National Laboratory,

Oak Ridge; Tennessee, 37831, USA

PACS: 77.80.Fm, 85.50.Gk, 77.84.Jd, 77.55.-g

Polarization reversal in ferroelectric nanomesas of polyvinylidene fluoride with trifluoroethylene PVDF-TrFE has been probed by ultrahigh vacuum piezoresponse force microscopy (PFM) in a wide temperature range from 89 to 326K. In a dramatic contrast to the macroscopic data, the PFM local switching was non-thermally-activated and, at the same time occurring at electric fields significantly lower than the intrinsic switching threshold. A "cold-field" defect-

mediated extrinsic switching is shown to be an adequate scenario describing this peculiar switching behavior. The extrinsic character of the observed polarization reversal suggests that there is no fundamental bar for lowering the coercive field in ferroelectric polymer nanostructures, which is of importance for their applications in functional electronics.

Ferroelectric polymers, in particular PVDF and its co-polymers offer an attractive combination of properties such as relatively high spontaneous polarization, piezoelectricity, electrical strength, chemically inert behavior and durability. These benefits together with benign processing demands explain the attention that PVDF-TrFE thin films receive, in particular for non-volatile memories and full-organic transistors[1-5]. Beyond conventional memory applications PVDF-TrFE layers can be integrated on a wide range of semiconductor systems enabling novel device functionalities. A spectacular example of this approach is the organic photovoltaic device with the charge separation enhanced by a ferroelectric polymer layer[6]. Another example from the field of multiferroics is the field-effect device where the ferromagnetism in a thin diluted magnetic semiconductor layer is controlled via the persistent field effect of the PVDF-TrFE ferroelectric gate[7].

Apart from the practical interest for functional electronics PVDF-TrFE represents a useful model system for exploring fundamentals of ferroelectricity. A unique combination of low dielectric constant and high spontaneous polarization results in a relatively weak depolarization effect, which permits to readily probe ferroelectricity in ultra-thin films with thickness of few monolayers, close to the fundamental limit of ferroelectricity. A peculiar switching behavior of ultra-thin PVDF-TrFE films

characterized by intrinsic switching kinetics has been reported[8], whereas thicker films show conventional extrinsic switching with thermally-activated dependence[9]. The differentiation between the intrinsic (reaching the spinodal on the temperature – electric field phase diagram) and extrinsic switching has been addressed in Refs.[8, 10] focused on polarization reversal analysis in PVDF-TrFE . Customarily, using the term "extrinsic switching" one implies the switching driven by nucleation of reverse domains assisted by thermal fluctuations, and subsequent domain wall motion. However, there exists a particular kind of extrinsic switching that is promoted by the defects of the material rather than by these fluctuations. In this scenario, the nucleolus of the reverse domain located at a defect becomes unstable when the electric field exceeds a certain threshold value. In other words, this mode of switching behavior occurs when the external electric field is high enough to completely suppress the potential barrier for the polarization domain nucleation[11]. This special case of extrinsic switching that we call after Ref.[11] "cold field switching" may look very similar to the true intrinsic switching, since in both cases the typical activation dependence of thermally activated switching is absent. However the difference between these two switching regimes is quite profound and can be of practical importance for PVDF and other systems with high coercive fields. Indeed, the intrinsic switching does not require any nucleation at all, whereas the cold field switching is still a nucleation-triggered process. Hence, in the case of cold-field switching the polarization reversal can be in principle enhanced via lowering the nucleation barrier by modifying the interface of the ferroelectric film and/or adding dopants etc. This approach is of practical interest for PVDF-TrFE films known for very high coercive voltage V_C representing a significant drawback for potential electronic applications.

Here we explore switching in PVDF mesas in the scanning probe tip geometry in a wide temperature range, and show that it is most adequately described by the cold field switching mechanism. For this study 77/23 PVDF-TrFE mesas with high degree of crystallinity have been prepared on Au-coated silicon substrate by spincoating using a 0.25% methyl ethyl ketone solution deposited at 2000 rpm. After annealing at 137°C/10min the thin polymer layer transforms into mesas with lateral size of 100-300 nm and height of 40-50 nm (Figure 1a). In addition to the ferroelectric mesas thin film capacitors with thickness of 100 nm have been fabricated for reference purposes. For these capacitors we used 2% solution fabricated from same precursors, same substrate and annealing profile as for nanomesas. 50 nm Au top electrodes with area of 3.2×10^{-3} cm^2 have been deposited by thermal evaporation. X-ray $\theta–2\theta$ scans performed on our PVDF-TrFE samples show clear peaks a 19.7°, which corresponds to (110) d-spacing of the all-trans ferroelectric β-phase. The high degree of cristallinity was further proved by measurements of saturating piezoelectric loops and sharp polarization hysteresis loops with the spontaneous polarization close to the maximal expected value (supplementary material provides further details).

The Polarization switching has been investigated at the temperature range from 89 to 326K under ultrahigh vacuum < 1E-9 Torr using commercial (Omicron) variable temperature scanning probe microscope modified for piezoresponse force microscopy.

Because of the complicated nature of charge transfer in PVDF-based polymers discrimination between the true ferroelectric switching and contributions due to the electret effects and dielectric relaxation may present additional difficulties. In order to avoid potential problems with obtaining accurate values of coercive voltages, surface strain due to applied DC electric field was directly measured instead of conventional

low signal piezoelectric response. In the strain curves representing the vertical displacement of the cantilever as a function of bias the coercive voltage, V_C is signaled by a maximum (or minimum) around the piezoelectric coercive field.

Figures 1(b-e) show typical strain curves measured at $89 - 326$K with triangular voltage wave with the period of 2s. Due to the negative longitudinal piezoelectric coefficient d_{33} the curve tips point downwards while V_C corresponds to the maximum unlike the common ferroelectric perovskites. The strain curve maxima uniquely identify the ferroelectric switching process in PVDF-TrFE as opposed to extrinsic processes related to charge injection or surface damage (which would be in general manifested as topographic changes). The quality of the single strain curves allowed to eliminate multiple loop collection with subsequent averaging, to avoid charge accumulation and electret memory effects that may influence V_C measurements. The single unprocessed strain loops shown in Figs. 1(b-e) illustrate a very high stability and low noise in this measurement.

The strain loops have been previously measured on PVDF-TrFE layers using parallel-plate capacitor geometry via the interferometer technique[12] and scanning tunneling microscope[13]. Both groups reported loops with abrupt change of strain near the coercive field. Compared to these data the strain loops in Fig. 1 (b-e) are much smoother and characterized by rounded peaks close to V_C. This difference is linked to the geometry of our experiment, where the piezoelectric properties are probed by the PFM tip, which serves as a top electrode. This technique provides very selective local switching within the region comparable with the tip radius (as opposed to the entire capacitor switching in Refs [12, 13]). On the other hand, the difficulty associated with this local probing technique is a non-uniform electric field, and consequently the switching characteristics are never as sharp as in the capacitor configuration.

The magnitude of measured strain proves that the complete polarization reversal has been achieved in the measurements shown in Fig 1(b-e). The value of transverse piezoelectric coefficient d_{33} in P(VDF-TrFE) with composition of 78/22 (nearly same composition as our material) quoted in Ref.[12] is 40 pm/V. Hence, application of 10V to the completely poled film results in a displacement of 4Å. This is very close to our room temperature data from Fig. 1, where 5Å displacement corresponds to the voltage change from 0 to 10V applied to the fully poled nanomesa. It is impossible to reach such a significant deformation by electrostriction in non-poled or partially poled films.

The strain amplitude decrease at lower temperatures observed in Fig. 1 also agrees with the piezoelectric effect. Indeed, the transverse piezoelectric coefficient is proportional to both dielectric constant and polarization, both being sensitive to the temperature. However, within the studied temperature range polarization is a relatively weak function of temperature while the dielectric constant changes quite significantly. In our measurements performed on the reference capacitor of dielectric constant dropped from 7.7 at 293K to 3.5 at 90K i.e. by factor 2.2 (as shown in Supplementary Material), this factor closely corresponds to the change of the amplitude of the strain curve observed in Fig. 1 at these temperatures.

A systematic study of temperature dependence of V_C has been performed by measuring strain curves on 20-50 different spots at each temperature and analyzing distribution of V_C for 8 temperature values within the range from 89K to 326K. Figure 1f representing Vc values obtained at temperatures of 89 K, 141K, 294K and 326 K shows a slight increase and broadening distribution of V_C with the temperature decease. The Vc data from the entire temperature range (Fig. 1g) attest to a weak non-acivation type temperature dependence of the coercive field in dramatic contrast with

the strongly temperature-dependent extrinsic switching typically observed in PVDF-TrFE in this thickness range. This prompts an interpretation in terms of intrinsic switching, however the switching data obtained for PVDF-TrFE films in parallel plate capacitor configuration do not agree with this scenario. Indeed, in Au/PVDF-TrFE/Au capacitors the coercive field extracted from the conventional P-E hysteresis loops (Fig. 2a, inset) shows nearly linear dependence on 1/T, in agreement with the theory for thermally-activated nucleation-controlled switching (Fig. 2a). This dependence holds at least up to 6MV/cm indicating that the thermodynamic coercive field exceeds 6MV/cm. On the other hand, the gold-plated cantilever tip with radius > 50 nm generates maximal electric field < 2 MV/cm, for the bias voltage of 10V (for details see Ref. [14] and Supplementary Material). In this case, in the SPM experiment the maximal electric field seen by the ferroelectric polymer is at least 3 times lower than the field of intrinsic switching. Thus the polarization reversal in nanomesas cannot be described by intrinsic switching. An adequate description of the switching process in this case is given by the cold field switching mechanism that combines the nucleation-controlled kinetics and weak temperature dependence seen in Fig. 1g.

The apparent discrepancy between the switching behavior of PVDF-TrFE nanomesas and capacitors needs to be separately addressed. Our interpretation relies on the following key assumptions: (i) cold-field switching mediated by defects occurs in the nanomesas as well in capacitors; (ii) in the capacitors the cold field switching results in a local polarization reversal in small areas (negligible compared to the capacitor area) without triggering the entire capacitor switching. The impossibility to switch the capacitor through the cold-field mechanism is explained by the secondary (amorphous) phase existing in a small quantity even in a well-crystallized film. The inclusions of the amorphous phase between the polymer grains produce barriers,

which impede switching at low temperature. In the previous work [15] we clearly observed by PFM in PVDF-TrFE capacitors some boundaries inhibiting the propagation of the switched state, which we attribute to this effect. Unlike capacitors the nanomesas represent compact islands composed of a small number of densely packed grains where the amorphous phase inclusions are more likely to concentrate close to the boundaries or outside the main cluster of polymer grains. Hence, cold field switching in the nanomesa results in the polarization reversal, while in the capacitor it switches only some isolated nano-scale areas, which are not noticeable when measuring the macroscopic hysteresis loops.

The shape of piezoelectric hysteresis loops is another differentiator that allows for discrimination between intrinsic switching and cold field switching. In the case of intrinsic switching, upon approaching the thermodynamic coercive field E_{th}, the electric field drives a given domain state of the ferroelectric to loose its stability. This implies a divergence of the small signal response to electric field, specifically, an anomalously high longitudinal piezoelectric coefficient d_{33} at the coercive field which, in this scenario, equals E_{th}. In contrast, extrinsic switching occurs at fields much smaller than E_{th}, so that no singularity of d_{33} at the coercive field of the loop is expected [16]. In reality, in view of finite amplitude of the measuring ac field, the aforementioned singularity will be smeared. However, if this amplitude is appreciably smaller than that of the ramping field of the loop, the intrinsic switching must reveal itself by a measurable increase of d_{33} on approaching the coercivity. We have employed this criterion for the analysis of our data. Figure 2b shows hysteresis loops of transverse piezoelectric coefficient d_{33} obtained via resonant band excitation technique[17] at 326K and 89K. In both cases the loops are characterized by a pronounced saturation behavior with no visible increase of d_{33} at the coercive voltage.

This can be considered as an additional argument in favor of cold-field switching scenario.

Further studies are required to identify the nature of defects responsible for the cold-field switching. The defects associated with the all-trans (β-phase) molecular conformation and molecular packing[18] can influence the switching kinetics in PVDF-TrFE nanomesas stabilizing residuals of the opposite domains especially in the crystallite extremities. Then these residuals may serve as nucleation centers for switching in the reverse direction via the cold-field switching mechanism.

In conclusion, polarization switching characterized by a weak non-activation-type temperature dependence has been observed in PVDF-TrFE mesas. The appealingly straightforward interpretation in terms of the intrinsic switching appears to be incompatible with the macroscopic data showing that within the studied range of electric fields the switching is purely extrinsic. An additional argument against the intrinsic switching is the piezoelectric loop shape, which does not agree with the intrinsic switching scenario. We show that the observed behavior of local polarization reversal is compatible with a particular kind of extrinsic switching promoted by the defects of the material rather than by the thermal fluctuations. In this switching mode, which occurs when the external electric field is high enough to completely suppress the domain nucleation potential barrier, the switching rate does not obey any thermally activated dependence of temperature similar to the classic intrinsic switching. However despite this similarity, the presented switching mechanism is fundamentally different from the true intrinsic switching since it relies on the nucleation centers. The important practical implication is a possibility to influence the switching properties via the introduction of artificial nucleation centers e.g. by doping and chemical or mechanical modification of the polymer film interface. Hence, the

high electric fields typically required to switch ferroelectric polymer films and nanostructures can be in principle lowered, which would make these materials even more attractive for electronic application.

References

1. R. C. G. Naber, C. Tanase, P. W. M. Blom, G. H. Gelinck, A. W. Marsman, F. J. Touwslager, S. Setayesh and D. M. De Leeuw, Nature Materials **4** (3), 243-248 (2005).

2. A. Gerber, M. Fitsilis, R. Waser, T. J. Reece, E. Rije, S. Ducharme and H. Kohlstedt, Journal of Applied Physics **107** (12), 124119 (2010).

3. T. Nakajima, Y. Takahashi, S. Okamura and T. Furukawa, Jpn J Appl Phys **48** (9), 09KE04 (2009).

4. X. B. Lu, J. W. Yoon and H. Ishiwara, Journal of Applied Physics **105** (8), 084101 (2009).

5. L. Malin, I. Stolichnov and N. Setter, Journal of Applied Physics **102** (11), 114101 (2007).

6. Y. B. Yuan, T. J. Reece, P. Sharma, S. Poddar, S. Ducharme, A. Gruverman, Y. Yang and J. S. Huang, Nature Materials **10** (4), 296-302 (2011).

7.   I. Stolichnov, S. W. E. Riester, H. J. Trodahl, N. Setter, A. W. Rushforth, K. W. Edmonds, R. P. Campion, C. T. Foxon, B. L. Gallagher and T. Jungwirth, Nature Materials **7** (6), 464-467 (2008).

8.   G. Vizdrik, S. Ducharme, V. M. Fridkin and S. G. Yudin, Physical Review B **68** (9), 094113 (2003).

9.   R. V. Gaynutdinov, O. A. Lysova, A. L. Tolstikhina, S. G. Yudin, V. M. Fridkin and S. Ducharme, Applied Physics Letters **92** (17), 172902 (2008).

10.   H. Kliem and R. Tadros-Morgane, Journal of Physics D-Applied Physics **38** (18), 3554-3554 (2005).

11.   G. Gerra, A. K. Tagantsev and N. Setter, Physical Review Letters **94** (10), 107602 (2005).

12.   T. Furukawa and N. Seo, Japanese Journal of Applied Physics Part 1-Regular Papers Short Notes & Review Papers **29** (4), 675-680 (1990).

13.   L. Jie, C. Baur, B. Koslowski and K. Dransfeld, Physica B **204** (1-4), 318-324 (1995).

14.   M. Molotskii, Journal of Applied Physics **93** (10), 6234-6237 (2003).

15.   R. Gysel, I. Stolichnov, A. Taganstev, N. Setter and P. Mokry, Journal of Applied Physics **103** (8), 084120 (2008).

16.   A. Tagantsev, E. Cross and J. Fousek, *Domains in ferroic crystals and thin films*. (Springer, New York, 2010).

17.   S. Jesse, S. V. Kalinin, R. Proksch, A. P. Baddorf and B. J. Rodriguez, Nanotechnology **18** (43), 435503 (2007).

18.   A. Gruverman, P. Sharma, T. J. Reece and S. Ducharme, Nano Letters **11** (5), 1970-1975 (2011).

Figure captions

Figure 1. (a) Topography image of PVDF-TrFE mesas deposited on the Au-coated silicon wafer and height profile measured along the dashed line. (b-e) Vertical displacement of the PFM cantilever vs. applied voltage (strain curves) measured on PVDF-TrFE mesas at 89K, 141K, 298K and 326K. The smoothness of the raw curves plotted as measured without any averaging attests to a good stability and low noise in this measurement. (f) Distributions of coercive voltage measured on 20-50 different spots at each temperature, for 89K, 141K, 298K and 326K. (g) Coercive voltage extracted from the strain curve maxima vs. temperature.

Figure 2. (a) Macroscopic data of coercive field vs. temperature extracted from P-V loops measured on Au/PVDF-TrFE/Au capacitors with different compositions and thickness of 110nm and 200nm. Inset: typical 10kHz P-V hysteresis loops used for the coercive field determination. (b) Local piezoelectric hysteresis loops measured on 50nm PVDF-TrFE mesas via resonant band excitation technique by PFM at 326K and at 89K.
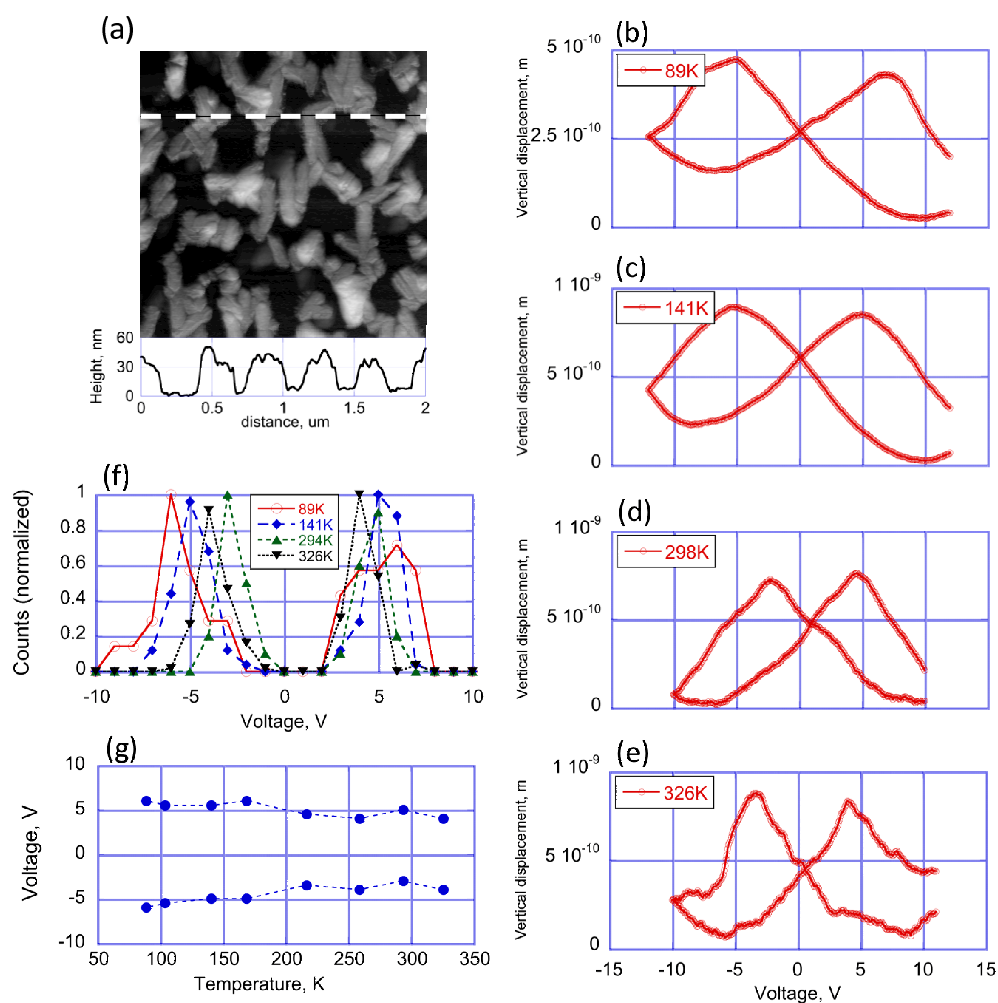
Figure 1. (a) Topography image of PVDF-TrFE mesas deposited on the Au-coated silicon wafer and hight profile measured along the dashed line. (b-e) Vertical displacement of the PFM cantilever vs. applied voltage (strain curves) measured on PVDF-TrFE mesas at 89K, 141K, 298K and 326K. The smoothness of the raw curves plotted as measured without any averaging attests to a good stability and low noise in this measurement. (f) Distributions of coercive voltage measured on 20-50 different spots at each temperature, for 89K, 141K, 298K and 326K. (g) Coercive voltage extracted from the strain curve maxima vs. temperature.
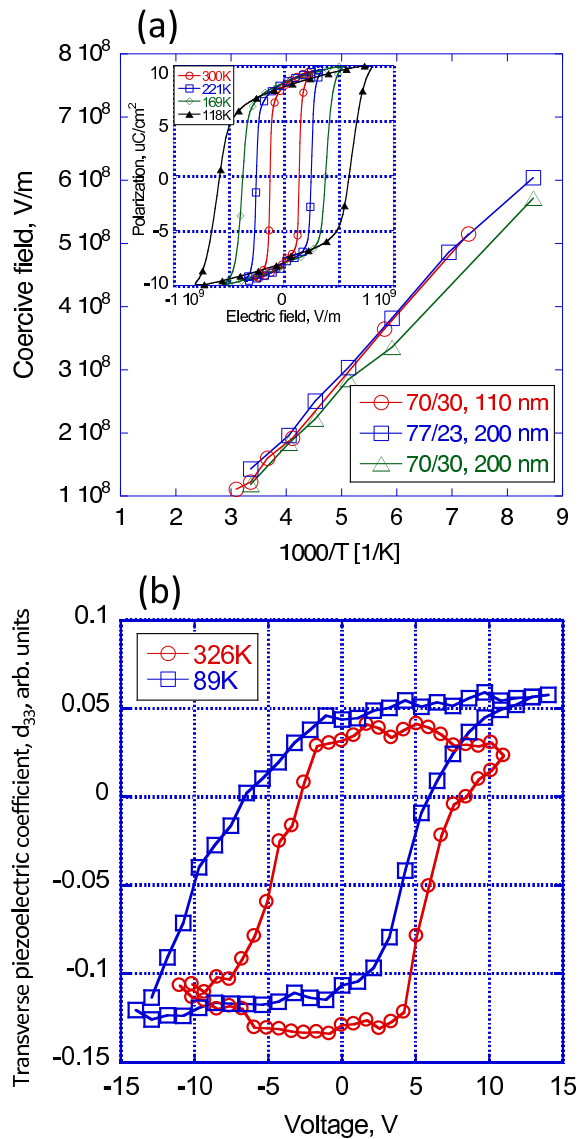
Figure 1   LG13336   23NOV2011

Figure 2. (a) Macroscopic data of coercive field vs. temperature extracted from P-V loops measured on Au/PVDF-TrFE/Au capacitors with different compositions and thickness of 110nm and 200nm. Inset: typical 10kHz P-V hysteresis loops used for the coercive field determination. (b) Local piezoelectric hysteresis loops measured on 50nm PVDF-TrFE mesas via resonant band excitation technique by PFM at 326K and at 89K.

Figure 2   LG13336   23NOV2011